Astronomy & Astrophysics manuscript no. Ballester
January 27, 2010

© ESO 2010

arXiv:1001.4962v1 [astro-ph.SR] 27 Jan 2010

The spatial damping of magnetohydrodynamic waves in a flowing partially ionised prominence plasma

M. Carbonell[1], P. Forteza[2], R. Oliver[2], and J. L. Ballester[2]

[1] Departament de Matemàtiques i Informàtica, Universitat de les Illes Balears, E-07122 Palma de Mallorca, Spain
[2] Departament de Física, Universitat de les Illes Balears, E-07122 Palma de Mallorca, Spain
e-mail: `marc.carbonell@uib.es; pepfortezaferrer@gmail.com; ramon.oliver@uib.es; joseluis.ballester@uib.es`

Received / Accepted

ABSTRACT

Context. Solar prominences are partially ionised plasmas displaying flows and oscillations. These oscillations show time and spatial damping and, commonly, have been explained in terms of magnetohydrodynamic (MHD) waves.

Aims. We study the spatial damping of linear non-adiabatic MHD waves in a flowing partially ionised plasma, having prominence-like physical properties.

Methods. We consider single fluid equations for a partially ionised hydrogen plasma including in the energy equation optically thin radiation, thermal conduction by electrons and neutrals, and heating. Keeping ω real and fixed, we have solved the obtained dispersion relations for the complex wavenumber, k, and have analysed the behaviour of the damping length, wavelength and the ratio of the damping length to the wavelength, versus period, for Alfvén, fast, slow and thermal waves.

Results. The results indicate that in presence of a background flow new strongly damped fast and Alfvén waves appear which depend on the joint action of flow and resistivity. The damping lengths of adiabatic fast and slow waves are strongly affected by partial ionisation, which also modifies the ratio between damping lengths and wavelengths. Moreover, the behaviour of adiabatic fast waves looks very similar to that of Alfvén waves. For non-adiabatic slow waves, the unfolding in wavelength and damping length induced by the flow, allows that an efficient damping can be found for periods compatible with those observed in prominence oscillations. This effect is enhanced when low ionised plasmas are considered.

Conclusions. Since flows are ubiquitous in prominences, in the case of non-adiabatic slow waves and within the range of periods of interest for prominence oscillations, the joint effect of both flow and partial ionisation leads to a ratio between damping length and wavelength denoting a very efficient spatial damping. For fast and Alfvén waves, the most efficient damping occurs at very short periods not compatible with those observed in prominence oscillations.

Key words. Sun: oscillations – Sun: magnetic fields– Sun: prominences

1. Introduction

A solar prominence is a cool ($T \sim 10^4$ K) and dense ($\rho \sim 5 \cdot 10^{11}$ kg/m^3) mass of gas located in the much denser and hotter solar corona. Although it is not well understood how this structure can live for a long time within the solar corona, it is thought that its support and thermal isolation are of magnetic origin. Thanks to ground and space-based observations, evidence about the presence of small-amplitude oscillations in prominences and filaments is now widely available and detailed information can be found in Oliver and Ballester (2002), Banerjee et al. (2007), Oliver, (2009), and Mackay et al. (2009). The oscillations are mainly detected through the periodic Doppler shifts of spectral lines, with periods from a few minutes to hours, and the observations have shown that they are of local nature, that they can be coherent over large regions of prominences/filaments, that simultaneously flowing and oscillating features are present, and that oscillations display time and spatial damping (Terradas et al. 2002). These small-amplitude oscillations have been commonly interpreted in terms of linear magnetohydrodynamic (MHD) waves and the damping of oscillations has been studied by considering different dissipative mechanisms. For instance, in the case of fully ionised plasmas the time damping of prominence oscillations has been studied by considering non-adiabatic MHD waves, including the effect of optically thin radiation, thermal conduction and heating, in unbounded and bounded prominence plasmas (Carbonell et al. 2004; Terradas et al. 2005); furthermore, assuming that the threads that seem to compose solar filaments can be modeled as cylindrical flux tubes, the time damping of homogeneous and inhomogeneous cylindrical flux tubes, with prominence physical conditions, has been modeled using thermal mechanisms and resonant absorption, respectively (Soler et al. 2008; Arregui et al. 2008; Soler et al. 2009b).

A typical feature in prominence oscillations is the presence of flows which are observed in $H\alpha$, UV and EUV lines (Labrosse et al. 2009). In $H\alpha$ quiescent filaments, the observed velocities range from 5 to 20 km/s (Zirker et al. 1998; Lin et al. 2003, 2007) and, because of physical conditions in filament plasma, they seem to be field-aligned. In the case of active region prominences, flow speeds can be higher. Recently, observations made with Hinode/SOT by Okamoto et al. (2007) reported the presence of synchronous vertical oscillatory motions in the threads of an active region prominence, together with the presence of flows along the same threads. However, in limb prominences different kinds of flows are observed and, for instance, observations made by Berger et al. (2008) with Hinode/SOT have revealed a complex dynamics with vertical downflows and upflows. Taking all this into account, Carbonell et al (2009) explored the time damping of non-adiabatic slow and thermal waves in an unbounded prominence medium with a background flow, while Soler et al. (2008, 2009a) investigated the time damping of the oscillations of an individual prominence thread and of a threaded prominence when both mass flows and non-adiabatic processes are considered.

Send offprint requests to: J. L. Ballester
e-mail: `joseluis.ballester@uib.es`

Although there is a large amount of observational evidence about the time damping of MHD waves propagating in coronal structures such as coronal loops or prominences, current observational information about the spatial damping of MHD waves in coronal structures is still scarce. Time damping is usually produced when an impulsive perturbation excites a medium and waves start to propagate, then, the wave amplitude decreases as the time goes by. Alternatively, if the medium is excited by a continuous driver with a fixed frequency, the spatial damping is detected by the decrease of the amplitude when the wave propagates. Since, probably, most of the phenomena exciting waves in solar structures are of impulsive origin rather than produced by continuous drivers, time damping of waves is more often observed.

Concerning spatial damping, De Moortel et al. (2002) and De Moortel & Hood (2003, 2004), using thermal conduction, compressive viscosity, gravitational stratification and field line divergence, studied the spatial damping of driven and non-driven slow MHD waves in coronal conditions, applying the obtained results to the case of standing and propagating slow waves in coronal loops observed with SOHO and TRACE. In the case of prominences, Terradas et al. (2002) analyzed small amplitude oscillations in a polar crown prominence reporting the presence of a plane propagating wave as well as an standing wave. The plane wave propagates in opposite directions with wavelengths of $67,500$ and $50,000$ km and phase speeds of 15 km s^{-1} and 12 km s^{-1}, while in the case of the standing wave, the estimated wavelength is of $44,000$ km and the phase speed of 12 km s^{-1}. These authors also reported that in the case of the propagating wave, which was interpreted as a slow MHD wave, the amplitude of the oscillations spatially decreases in a substantial way in a distance of $2-5\times10^4$ km from the location where wave motion was being generated. This distance can be considered as a typical spatial damping length, L_{d}, of the oscillations.

From the theoretical point of view, and assuming a fully ionised plasma, Ballai (2003) performed a qualitative study of the spatial damping of linear compressional waves in solar prominences by considering different dissipative mechanisms such as isotropic and anisotropic viscosity, isotropic magnetic diffusivity, isotropic radiative damping (Newton's law) and anisotropic thermal conduction. The conclusion was that thermal radiation can damp compressional waves as well as that waves can be also damped by anisotropic thermal conduction provided that they have enough short wavelengths. Using linear non-adiabatic MHD waves, which included optically thin radiation, thermal conduction and heating, Carbonell et al. (2006) made a quantitative study of the spatial damping of slow, fast and thermal waves in a fully ionised unbounded prominence medium. In the frequency space, they determined the regions where radiation or thermal conduction are the dominant damping mechanisms, the critical frequencies at which the dominance changes from one mechanism to another, and the fact that different heating mechanisms do not strongly affect the damping. The most important conclusions were that the thermal wave is propagating but strongly damped, and that slow waves are efficiently damped by thermal effects, which does not happen for fast waves. Singh et al. (2006) did a similar study but considering only Newtonian radiation and, later, Singh et al. (2007) considered again the same problem including Newtonian radiation and turbulent viscosity.

The typical composition of solar prominences is 90% hydrogen and 10% helium and they constitute partially ionised plasmas since hydrogen lines are observed (Labrosse et al. 2009). The exact ionisation degree of prominences is unknown and the ratio of electron density to neutral hydrogen density seems to be in the interval $0.1-10$ (Patsourakos and Vial, 2002). From a theoretical point of view, partial ionisation was already considered by Mercier and Heyvaerts (1977) when they studied the difussion of neutral atoms due to gravity; also, Gilbert et al. (2002) studied the diffusion of neutral atoms in a partially ionized prominence plasma, concluding that the loss time scale is much longer for hydrogen than for helium. Recently, Gilbert et al. (2007) have investigated the temporal and spatial variations of the relative abundance of helium with respect to hydrogen in a sample of filaments. They have found that a majority of filaments show a deficit of helium in the top part while in the bottom part there is an excess. This seems to be due to the shorter loss time scale of neutral helium compared to that of neutral hydrogen. The consideration of prominences as made of partially ionised plasma is extremely important for the physics of prominences, and the effects on MHD waves in prominences need to be taken into account. From the theoretical point of view, and in the framework of laboratory plasma physics, a extense literature about wave propagation in a partially ionized multifluid plasma can be found (Watanabe, 1961a,b; Tanenbaum, 1961; Tanenbaum and Mintzer, 1962; Woods, 1962; Kulsrud and Pearce, 1969; Watts and Hanna, 2004). In astrophysical plasmas, the typical frequency of MHD waves is much smaller than the collisional frequencies between species. In such a case the single fluid approach is usually adopted and it has been applied to wave damping in the solar atmosphere (De Pontieu, et al. 2001; Khodachenko et al. 2004; Leake et al. 2005). In the case of solar prominences, Forteza et al. (2007) derived the full set of MHD equations for a partially ionized, single fluid plasma and applied them to study the time damping of linear, adiabatic waves in an unbounded prominence medium. Later, this study was extended to the non-adiabatic case by including thermal conduction by neutrals and electrons, radiative losses and heating (Forteza et al. 2008). Because of the effect of neutrals, in particular that of ion-neutral collisions, a generalized Ohm's law has to be considered, which causes some additional terms to appear in the resistive magnetic induction equation in comparison to the fully ionized case. Among these additional terms, the dominant one in the linear regime is the so-called ambipolar magnetic diffusion, which enhances magnetic diffusion across magnetic field lines. Furthermore, one of the interesting effects produced by the consideration of partial ionisation and ion-neutral collisions is that Alfvén waves can be damped, which cannot be obtained by means of thermal mechanisms, and Singh & Krishnan (2009) have studied the time damping of Alfvén-like waves in a partially ionised plasma representing a particular model of the solar atmosphere. For bounded media, Soler et al. (2009c) have applied this formalism to the study of the time damping of fast, Alfvén and slow waves in a partially ionised filament thread modeled as a cylinder, and Soler et al. (2009d) have used a cylindrical filament thread, having an inhomogeneous transition layer between prominence and coronal material, to study the influence of partial ionisation on the time damping of fast kink waves which is caused by resonant absorption in the inhomogeneous layer.

Up to now, and to our knowledge, no study of the spatial damping of MHD waves in a partially ionised plasma has been performed. Therefore, since solar prominences are partially ionised plasmas in which material flows and oscillations are present and since commonly these oscillations are interpreted in terms of MHD waves, our main aim here is to explore the theoretical and observational effects associated to the spatial damping of non-adiabatic MHD waves in an unbounded and partially ionised plasma, with prominence-like physical conditions, when a background flow is present. The layout of the paper is as follows: In Sect. 2, the equilibrium model and some theoretical considerations are presented; in Sect. 3, the spatial damping of Alfvén waves is studied; in Sect. 4, the spatial damping of magnetoacoustic waves is considered; finally, in Sect. 5, conclusions are drawn.

2. Model and Methods

2.1. Equilibrium Properties

As a background model, we use a homogeneous unbounded medium threaded by a uniform magnetic field along the x-direction, and with a field-aligned background flow. The equilibrium magnitudes of the medium are given by

$$p_0 = \text{const.}, \quad \rho_0 = \text{const.}, \quad T_0 = \text{const.},$$

$$\mathbf{B_0} = B_0 \hat{x}, \quad \mathbf{v}_0 = v_0 \hat{x},$$

with B_0 and v_0 constants, and the effect of gravity has been ignored. Since we consider a medium with physical properties akin to those of a solar prominence, the density is $\rho_0 = 5 \times 10^{-11}$ kg/m^3, the temperature $T_0 = 8000$ K, the magnetic field $|\mathbf{B}_0| = 10$ G, and, in general, a field-aligned flow with $v_0 = 10$ km/s, simulating the typical flows found in quiescent filaments, has been considered.

2.2. Basic and Linearised Equations

The derivation of the single-fluid MHD equations for a partially ionised hydrogen plasma can be found in Forteza et al. (2007). Later, these equations were modified in order to include non-adiabatic processes in the energy equation (Forteza et al. 2008), and the physical meaning of all the terms and quantities used in the following can be found in those papers. When a background flow is considered, the single fluid basic equations for the study of non-adiabatic MHD waves in a partially ionised plasma can be derived from Forteza et al. (2007, 2008) and Carbonell et al. (2009). The most important difference with respect to the non-adiabatic case without a background flow is that instead of the operator $\frac{\partial}{\partial t}$ we will have $\frac{\partial}{\partial t} + \mathbf{v}_0 \cdot \nabla$ in the MHD equations (Goedbloed and Poedts, 2004). Before proceeding, some remarks are in order: We consider a partially ionised hydrogen plasma characterized by a plasma density, ρ_0, temperature, T_0, and number densities of neutrals, n_n, ions, n_i, and electrons n_e, with $n_e = n_i$. Thus, the gas pressure is $p_0 = (2n_i + n_n) k_\mathrm{B} T_0$, where k_B is Boltzmann's constant. The relative densities of neutrals, ξ_n, and ions, ξ_i, are given by

$$\xi_n = \frac{n_n}{n_i + n_n}, \qquad \xi_i = \frac{n_i}{n_i + n_n}, \tag{1}$$

where we have neglected the contribution of electrons. We can now define a ionization fraction, $\tilde{\mu}$, which gives us information about the plasma degree of ionization,

$$\tilde{\mu} = \frac{1}{1+\xi_i}. \tag{2}$$

and the quantity

$$\Xi = \frac{\xi_n^2 \xi_i}{(1+\xi_i)\alpha_n}. \tag{3}$$

where α_n is a friction coefficient (Braginskii, 1965; Khodachenko et al. 2004; Leake et al. 2005). For a fully ionised plasma $\tilde{\mu} = 0.5$ while for a neutral plasma $\tilde{\mu} = 1$. Depending on the value given to $\tilde{\mu}$ and to Spitzer's (η) and Cowling's (η_{C}) resistivities, we may have different types of plasmas: A fully ionised ideal plasma (FIIP) is characterised by $\tilde{\mu} = 0.5$, $\eta = \eta_{\mathrm{C}} = \Xi = 0$; a fully ionised resistive plasma (FIRP) is characterised by $\tilde{\mu} = 0.5$, $\eta = \eta_{\mathrm{C}}$ and $\Xi = 0$; and a partially ionised plasma (PIP) is characterised by $\tilde{0}.5 < \tilde{\mu} < 1$, $\eta \neq \eta_{\mathrm{C}}$ and $\Xi \neq 0$. Although our main aim is the study of spatial damping of MHD waves in PIP, the case of FIRP will be also considered since it has received almost no attention in the literature. Another important issue for our study is the numerical value and behaviour of the sound (c_{s}) and Alfvén speeds (v_{a}). For fixed the density and magnetic field, the Alfvén speed has a constant numerical value of 126.15 km/s, however, since the sound speed depends on gas pressure, which is a function of the number densities of ions and neutrals, its numerical value is not constant but depends on the ionisation fraction considered. For a fully ionised plasma, the sound speed is 14.84 km/s while for a partially ionised plasma with $\tilde{\mu} = 0.95$ its value decreases to 10.76 km/s. This variation in the sound speed can be important since depending on the flow speed and ionisation fraction chosen, the flow speed could be greater than, smaller than or equal to the sound speed which affects the direction of propagation of slow and thermal waves (Carbonell et al. 2009). In our case, the flow speed is subsonic and subalfvénic which seems to be a typical feature of flows observed in quiescent filaments.

Next, to obtain the dispersion relation for linear MHD waves, we consider small perturbations from the equilibrium of the form

$$\begin{aligned}
&\boldsymbol{B}(t,\boldsymbol{r}) = \boldsymbol{B}_0 + \boldsymbol{B}_1(t,\boldsymbol{r}), \qquad p(t,\boldsymbol{r}) = p_0 + p_1(t,\boldsymbol{r}),\\
&\rho(t,\boldsymbol{r}) = \rho_0 + \rho_1(t,\boldsymbol{r}), \qquad T(t,\boldsymbol{r}) = T_0 + T_1(t,\boldsymbol{r}),\\
&\boldsymbol{v}(t,\boldsymbol{r}) = \boldsymbol{v}_0 + \boldsymbol{v}_1(t,\boldsymbol{r}).
\end{aligned}$$

and we linearise the single fluid basic equations. Since the medium is unbounded, we perform a Fourier analysis in terms of plane waves and assume that perturbations behave as

$$f_1(\boldsymbol{r},t) = f e^{i(\omega t - \boldsymbol{k}\cdot\boldsymbol{r})}. \tag{4}$$

and with no loss of generality, we choose the z-axis so that the wavevector $\boldsymbol{k}$ lies in the xz-plane ($\boldsymbol{k} = k_x\hat{\boldsymbol{x}} + k_z\hat{\boldsymbol{z}}$), and introducing the propagation angle, θ, between $\boldsymbol{k}$ and $\boldsymbol{B}_0$, the wavenumber components can be expressed as $k_x = k\cos\theta$ and $k_z = k\sin\theta$. With this approach, the operator $\frac{\partial}{\partial t} + \mathbf{v}_0 \cdot \nabla$ becomes $i(\omega - k_x v_0)$, which points out that in the presence of a background flow the frequency has a Doppler shift given by $k_x v_0$ and that the wave frequency, ω, for the non-adiabatic case with flow can be obtained from

$$\omega = \Omega + k_x v_0, \tag{5}$$

Ω being the wave frequency for the non-adiabatic case without flow. Also, these frequencies can be described in a different manner, Ω corresponds to the frequency measured by an observer linked to the flow inertial rest frame, while ω would correspond to the frequency measured by an observer linked to an external inertial rest frame.

After the Fourier analysis, the following linearised scalar equations are obtained.

$$\Omega\rho_1 - \rho_0(k_x v_{1x} + k_z v_{1z}) = 0, \tag{6}$$

$$\Omega\rho_0 v_{1x} - k_x p_1 = 0, \tag{7}$$

$$\Omega\rho_0 v_{1y} + \frac{B_{0x}}{\mu} k_x B_{1y} = 0, \tag{8}$$

$$\Omega\rho_0 v_{1z} - k_z p_1 + \frac{B_{0x}}{\mu}(k_x B_{1z} - k_z B_{1x}) = 0, \tag{9}$$

$$\begin{aligned} &i\Omega\left(p_1 - c_{\mathrm{s}}^2\rho_1\right) + (\gamma-1)\left(\kappa_{\mathrm{e}\parallel}k_x^2 + \kappa_{\mathrm{n}}k^2 + \rho_0 L_T\right)T_1 + \\ &\qquad\qquad +(\gamma-1)(L + \rho_0 L_\rho)\rho_1 = 0, \end{aligned} \tag{10}$$

$$\begin{aligned} &B_{1x}\left(i\Omega + k_x^2\eta + k_z^2\eta_{\mathrm{C}}\right) + (\eta - \eta_{\mathrm{C}})k_x k_z B_{1z} - \\ &\qquad\qquad -B_{0x}k_z(iv_{1z} - k_z\Xi p_1) = 0, \end{aligned} \tag{11}$$

$$B_{1y}\left(i\Omega + k_x^2\eta_{\mathrm{C}} + k_z^2\eta\right) + iB_{0x}k_x v_{1y} = 0, \tag{12}$$

$$\begin{aligned} &B_{1z}\left(i\Omega + k_x^2\eta_{\mathrm{C}} + k_z^2\eta\right) + (\eta - \eta_{\mathrm{C}})k_x k_z B_{1x} + \\ &\qquad\qquad +B_{0x}k_x(iv_{1z} - k_z\Xi p_1) = 0, \end{aligned} \tag{13}$$

$$k_x B_{1x} + k_z B_{1z} = 0, \tag{14}$$

$$\frac{p_1}{p_0} - \frac{\rho_1}{\rho_0} - \frac{T_1}{T_0} = 0. \tag{15}$$

2.3. Dispersion relation for Alfvén waves

Equations (8) and (12) are decoupled from the rest and from them we can obtain a dispersion relation for Alfvén waves in a partially ionised plasma with a background flow, which is,

$$\Omega^2 - i\Omega k^2(\eta_{\mathrm{C}}\cos^2\theta + \eta\sin^2\theta) - v_{\mathrm{a}}^2 k^2\cos^2\theta = 0 \tag{16}$$

where θ is the angle between the wavenumber vector and the magnetic field. In absence of flow, Eq. (16) reduces to,

$$k^2 = \frac{\omega^2}{\Gamma(\theta)^2\cos^2\theta}, \tag{17}$$

where $\Gamma(\theta)$ is a modified and complex Alfvén speed ($\Gamma(\theta) = \Gamma_{\mathrm{r}} + i\Gamma_{\mathrm{i}}$) defined as

$$\Gamma(\theta)^2 = v_{\mathrm{a}}^2 + i\omega\left(\eta_{\mathrm{C}} + \eta\tan^2\theta\right). \tag{18}$$

which was introduced by Forteza et al. (2008). In the case of a fully ionised ideal plasma without a background flow Eq. (16) reduces to the well known expression for Alfvén waves.

2.4. Dispersion relation for magnetoacoustic waves

From the remaining linearised equations, imposing that the determinant of the algebraic system be zero, we obtain our general dispersion relation for thermal and magnetoacoustic waves in presence of a background flow, which is given by,

$$\begin{aligned}(\Omega^2 - k^2\Lambda^2)(ik^2\eta_{\mathrm{C}}\Omega - \Omega^2) + k^2 v_{\mathrm{a}}^2(\Omega^2 - k_x^2\Lambda^2) + \\ + ik^2k_z^2v_{\mathrm{a}}^2\Lambda^2\Xi\rho_0\Omega = 0\end{aligned} \tag{19}$$

where Λ^2 is the non-adiabatic sound speed squared (Forteza et al. 2008, Soler et al. 2008) and is defined as

$$\Lambda^2 = \frac{\frac{T_0}{\rho_0}A - H + ic_{\mathrm{s}}^2\Omega}{\frac{T_0}{p_0}A + i\Omega} \tag{20}$$

where A and H, including optically thin radiative losses, thermal conduction by electrons and neutrals, and a constant heating per unit volume, are defined in Forteza et al. (2008). When Eq. (19) is expanded, it becomes a seventh degree polynomial in the wavenumber k. By setting the appropiate values to the corresponding quantities, the dispersion relation (19) is consistent with the case of an adiabatic and partially ionised plasma without flow (Forteza et al. 2007), the case of a non-adiabatic and partially ionised plasma without flow (Forteza et al. 2008) and the case of a non-adiabatic, fully ionised plasma with a background flow (Carbonell et al. 2009).

3. Spatial damping of Alfvén waves in a partially ionised plasma

Since we are interested in the spatial damping of MHD waves we consider the frequency, ω, to be real and seek for complex solutions of the wavenumber k expressed as $k = k_{\mathrm{r}} + ik_{\mathrm{i}}$. The wavelength of the waves is given by $\lambda = \frac{2\pi}{k_{\mathrm{r}}}$, the damping length by $L_{\mathrm{d}} = \frac{1}{k_{\mathrm{i}}}$ and the damping length per wavelength is $\frac{L_{\mathrm{d}}}{\lambda}$ and, in general, we consider a propagation angle $\theta = \frac{\pi}{4}$.

3.1. Spatial damping of Alfvén waves without background flow

In this case, our governing dispersion relation is given by Eq. (17), and the wavenumbers are

$$k = \pm\sqrt{\frac{(\omega\sec\theta)^2}{v_{\mathrm{a}}^2 + i\omega(\eta_{\mathrm{C}} + \eta\tan^2\theta)}} \tag{21}$$

representing two Alfvén waves propagating in opposite directions. The real part (k_r) of these wavenumbers is,

$$k_{\mathrm{r}} = \omega\sec\theta\frac{\sqrt{v_{\mathrm{a}}^2 + \sqrt{v_{\mathrm{a}}^4 + \omega^2(\eta_{\mathrm{C}} + \eta\tan^2\theta)}}}{\sqrt{2\left[v_{\mathrm{a}}^4 + \omega^2(\eta_{\mathrm{C}} + \eta\tan^2\theta)\right]}} \tag{22}$$

while the imaginary part (k_i) is,

$$k_{\mathrm{i}} = \frac{-\omega^2\sec\theta}{\sqrt{2\left[v_{\mathrm{a}}^4 + \omega^2(\eta_{\mathrm{C}} + \eta\tan^2\theta)\right]}}\times$$

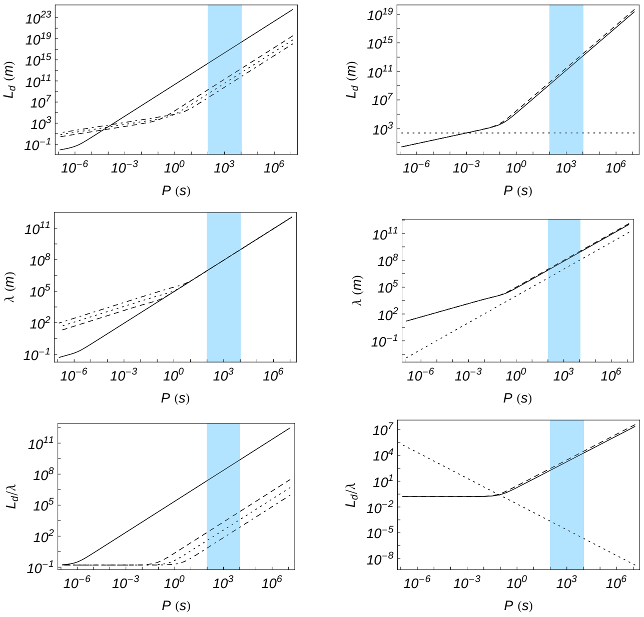

Fig. 1. Left panels: Damping length, wavelength, and ratio of the damping length to the wavelength versus the period for Alfvén waves in a FIRP (solid) and in PIP with $\tilde{\mu} = 0.8$ (dashed), $\tilde{\mu} = 0.95$ (dotted), and $\tilde{\mu} = 0.99$ (dash-dotted). Right panels: Damping length, wavelength, and ratio of the damping length to the wavelength versus period for the three (solid, dashed, dotted) Alfvén waves in a PIP with $\tilde{\mu} = 0.8$ and with a background flow of 10 km/s. In all the Figures, the shaded region corresponds to the interval of observed periods in prominence oscillations.

$$\times \frac{(\eta_{\mathrm{C}} + \eta \tan^2\theta)}{\sqrt{v_{\mathrm{a}}^2 + \sqrt{v_{\mathrm{a}}^4 + \omega^2(\eta_{\mathrm{C}} + \eta \tan^2\theta)}}} \tag{23}$$

Figure 1 (Left panels) shows a plot of the damping length, wavelength, and the ratio of the damping length to wavelength, versus the period, for Alfvén waves. The plots have been made for four different ionisation fractions and the shaded region corresponds to the interval of observed periods in prominence oscillations. When a period within the shaded region is considered, we observe that the damping length decreases in a substantial way when the amount of neutrals in the plasma increases. Then, when ion-neutral collisions are present the spatial damping of Alfvén waves is enhanced for periods greater than 1 s. Also, we can observe that for a FIRP the behaviour of the damping length, wavelength and their ratio versus period is linear, except for periods below 10^{-6} s. However, when a PIP is considered a deviation from the linear behaviour appears for periods below 1 s. This is due to the joint effect of the terms including frequency and resistivities in the real (k_r) and imaginary (k_i) parts of the wavenumber k since going to shorter periods frequency increases and its role becomes more important. The spatial damping of Alfvén waves in PIP with physical properties like those of quiescent prominences is very efficient for periods below 1 s, however, within the interval of periods of interest for prominence oscillations, it is only efficient, ($\frac{L_{\mathrm{d}}}{\lambda} \sim 1 - 10$), when almost neutral plasmas are considered.

3.2. Spatial damping of Alfvén waves with background flow

Now, our dispersion relation is given by Eq. (16) which once expanded becomes a cubic polynomial in the wavenumber k, such as,

$$\begin{aligned} i v_0(\eta_\mathrm{C}\cos^2\theta+\eta\sin^2\theta)k^3 &+ \\ +\left[(v_0^2-v_\mathrm{a}^2-i\eta_\mathrm{C}\omega)\cos\theta-i\eta\omega\sin\theta\tan\theta\right]k^2-2\omega v_0 k &+ \\ +\omega^2\sec\theta=0, \end{aligned} \tag{24}$$

The increase in the degree of the dispersion relation, with respect to the case without flow, is produced by the joint presence of flow and resistivities. In this case, we should obtain three propagating Alfvén waves, therefore, Figure 1 (Right panels) shows the numerical solution of dispersion relation (24) for the three Alfvén waves in a partially ionised plasma with a background flow. For all the interval of periods considered, a strongly damped third Alfvén wave appears, while on the contrary, and like in 3.1, the other two Alfvén waves are very efficiently damped for periods below 1 s. However, within the interval of periods typically observed in prominence oscillations these waves are only efficiently attenuated when almost neutral plasmas are considered. Furthermore, the following approximations for the different wavenumbers corresponding to two of the expected Alfvén waves can be calculated,

$$k\simeq\pm\sqrt{\frac{(\omega\sec\theta)^2}{(v_0\pm v_\mathrm{a})^2+i\omega(\eta_\mathrm{C}+\eta\tan^2\theta)}} \tag{25}$$

whose real part (k_r) is given by,

$$k_\mathrm{r}\ \simeq\ \omega\sec\theta\frac{\sqrt{(v_0\pm v_\mathrm{a})^2+\sqrt{(v_0\pm v_\mathrm{a})^4+\omega^2(\eta_\mathrm{C}+\eta\tan^2\theta)}}}{\sqrt{2\left[(v_0\pm v_\mathrm{a})^4+\omega^2(\eta_\mathrm{C}+\eta\tan^2\theta)\right]}} \tag{26}$$

while the imaginary part (k_i) is,

$$\begin{aligned} k_\mathrm{i}\ &\simeq\ \frac{-\omega^2\sec\theta}{\sqrt{2\left[(v_0\pm v_\mathrm{a})^4+\omega^2(\eta_\mathrm{C}+\eta\tan^2\theta)\right]}}\times \\ &\times\frac{(\eta_\mathrm{C}+\eta\tan^2\theta)}{\sqrt{(v_0\pm v_\mathrm{a})^2+\sqrt{(v_0\pm v_\mathrm{a})^4+\omega^2(\eta_\mathrm{C}+\eta\tan^2\theta)}}} \end{aligned} \tag{27}$$

From the above expressions, if we consider a FIIP we recover the dispersion relation for Alfvén waves with a background flow (Carbonell et al. 2009), and if we remove the flow, the well-known dispersion relation for Alfvén waves is recovered. Since the flow speed is much smaller than the Alfvén speed, the effect of the flow on the real and imaginary parts of the wavenumber is very small, then, the wavelengths and damping lengths are similar to those in 3.1. The third remaining wavenumber of Eq. (24) can be approximated by,

$$k=\frac{\omega}{v_0\cos\theta}+i\frac{(v_0^2-v_\mathrm{a}^2)\cos\theta}{v_0(\eta_\mathrm{C}\cos^2\theta+\eta\sin^2\theta)}, \tag{28}$$

corresponding to the third Alfvén wave. All the above analytical approximations display an excellent agreement with the numerical results, and the presence of the third Alfvén wave, given by Eq. (28), fully depends on the join presence of flow and resistivities since, otherwise, the dispersion relation (24) would be quadratic. For an external observer to the flowing plasma, this additional wave could be detectable, although its strong spatial damping would make its detection very difficult. For an observer linked to the flow inertial rest frame, only the two usual Alfvén waves, modified by resistivities, would be detected.

4. Spatial damping of Magnetoacoustic waves in a partially ionised plasma

Our general dispersion relation for non-adiabatic magnetoacoustic waves in presence of a background flow is given by Eq. (19). Because of the complexity of this dispersion relation, and in order to be able to understand the results, we have split our study in a sequence of four different cases having dispersion relations of increasing complexity. In the first two cases, the behaviour of adiabatic magnetoacoustic waves in a non-flowing (4.1) and flowing plasma (4.2) is considered; while in the last two cases, the behaviour of non-adiabatic waves in a non-flowing (4.3) and flowing plasma (4.4) is studied.

4.1. Adiabatic Magnetoacoustic waves without background flow

Setting $A = H = 0$ in Eq. (20), $v_0 = 0$ in expression (5) and substituting in Eq. (19), we obtain the dispersion relation for adiabatic magnetoacoustic waves in a PIP without a background flow, which is

$$(\omega^2 - k^2 c_{\rm s}^2)(ik^2\eta_{\rm C}\omega - \omega^2) + k^2 v_{\rm a}^2(\omega^2 - k_x^2 c_{\rm s}^2) + ik^2 k_z^2 v_{\rm a}^2 c_{\rm s}^2 \Xi \rho_0 \omega = 0 \qquad (29)$$

already found by Forteza et al. (2007)

4.1.1. Fully ionised resistive plasma

Now, imposing FIRP conditions from 2.2, the dispersion relation (29) simplifies to,

$$(\omega^2 - k^2 c_{\rm s}^2)(ik^2\eta\omega - \omega^2) + k^2 v_{\rm a}^2(\omega^2 - k_x^2 c_{\rm s}^2) = 0 \qquad (30)$$

which once expanded gives a fourth degree polynomial in the wavenumber k,

$$k^4 c_{\rm s}^2(\cos^2\theta\, v_{\rm a}^2 + i\omega\eta) - k^2\omega^2(c_{\rm s}^2 + v_{\rm a}^2 + i\omega\eta) + \omega^4 = 0. \qquad (31)$$

Furthermore, when only longitudinal propagation is allowed ($\theta = 0$), dispersion relation (30) can be factorized as

$$(\omega^2 - k^2 c_{\rm s}^2)\left[\omega^2 - k^2(v_{\rm a}^2 + i\omega\eta)\right] = 0 \qquad (32)$$

giving place to two undamped slow waves with a dispersion relation given by,

$$k^2 = \frac{\omega^2}{c_{\rm s}^2}$$

and, since for longitudinal propagation fast waves become Alfvén waves, we obtain two Alfvén waves, damped by resistivity, whose dispersion relation is,

$$k^2 = \frac{\omega^2}{v_{\rm a}^2 + i\eta\omega}$$

For these Alfvén waves, the real (k_r) and imaginary (k_i) parts of the wavenumber k can be obtained from expressions (22) and (23) setting $\theta = 0$. Then, in the case of a FIRP, when oblique propagation is not allowed, resistivity does not affect slow waves, which propagate undamped, and only affects fast waves. Next, if we allow oblique propagation ($0 < \theta < \pi/2$) in dispersion relation (31), the solutions for the wavenumbers are given by,

$$k_{\mathrm{m}}^2 = \frac{\omega^2(v_{\mathrm{a}}^2 + c_{\mathrm{s}}^2 + i\eta\omega)}{2ic_{\mathrm{s}}^2(\eta\omega - iv_{\mathrm{a}}^2\cos^2\theta)} + \\ + \frac{\omega^2\sqrt{(v_{\mathrm{a}}^2 + c_{\mathrm{s}}^2 + i\eta\omega)^2 - 4ic_{\mathrm{s}}^2(\eta\omega - iv_{\mathrm{a}}^2\cos^2\theta)}}{2ic_{\mathrm{s}}^2(\eta\omega - iv_{\mathrm{a}}^2\cos^2\theta)} \tag{33}$$

and

$$k_{\mathrm{n}}^2 = \frac{\omega^2(v_{\mathrm{a}}^2 + c_{\mathrm{s}}^2 + i\eta\omega)}{2ic_{\mathrm{s}}^2(\eta\omega - iv_{\mathrm{a}}^2\cos^2\theta)} - \\ - \frac{\omega^2\sqrt{(v_{\mathrm{a}}^2 + c_{\mathrm{s}}^2 + i\eta\omega)^2 - 4ic_{\mathrm{s}}^2(\eta\omega - iv_{\mathrm{a}}^2\cos^2\theta)}}{2ic_{\mathrm{s}}^2(\eta\omega - iv_{\mathrm{a}}^2\cos^2\theta)} \tag{34}$$

where k_{m}^2 and k_{n}^2 are the wavenumbers corresponding to two coupled and damped fast and slow waves propagating in opposite directions. Figure 2 displays the behaviour of damping length, wavelength and the ratio of damping length to wavelength versus period for fast and slow waves, respectively. In these figures it is clearly observed that the behaviour of the wavelength is the same for a FIRP and a FIIP, and that the only difference occurs at periods below 10^{-6} s due to resistivity. However, looking to the ratio of the damping length to the wavelength, we can conclude that in a FIRP, and within the interval of periods of interest, the spatial damping of both waves is negligible.

4.1.2. Partially ionised plasma

The dispersion relation is given by Eq. (29), and considering only longitudinal propagation we obtain,

$$(\omega^2 - k^2c_{\mathrm{s}}^2)\left[\omega^2 - k^2(v_{\mathrm{a}}^2 + i\omega\eta_{\mathrm{C}})\right] = 0 \tag{35}$$

This could suggest that the consideration of longitudinal propagation in a FIRP or in a PIP leads to the same dispersion relation, however, there is an important difference, while for FIRP both resistivities have the same numerical value, for PIP the numerical value of Cowling's resistivity is much greater than that of Spitzer's resistivity. Furthermore, for longitudinal propagation the slow waves are not influenced by Cowling's resistivity. Once expanded, Eq. (35) gives the following fourth degree polynomial in the wavenumber k,

$$k^4ic_{\mathrm{s}}^2\left[\eta_{\mathrm{C}}\omega - iv_{\mathrm{a}}^2\cos^2\theta + v_a^2\rho_0\omega\Xi(\cos^2\theta - 1)\right] - \\ -k^2\omega^2(v_{\mathrm{a}}^2 + c_{\mathrm{s}}^2 + i\eta_{\mathrm{C}}\omega) + \omega^4 = 0. \tag{36}$$

After solving this biquadratic dispersion relation, we obtain,

$$k_{\mathrm{m}}^2 = \frac{A + \sqrt{B}}{C} \tag{37}$$

$$k_{\mathrm{n}}^2 = \frac{A - \sqrt{B}}{C} \tag{38}$$

with

$$A = (v_{\mathrm{a}}^2 + c_{\mathrm{s}}^2 + i\eta_{\mathrm{C}}\omega)$$

$$B = (v_{\mathrm{a}}^2 + c_{\mathrm{s}}^2 + i\eta_{\mathrm{C}}\omega)^2 -$$

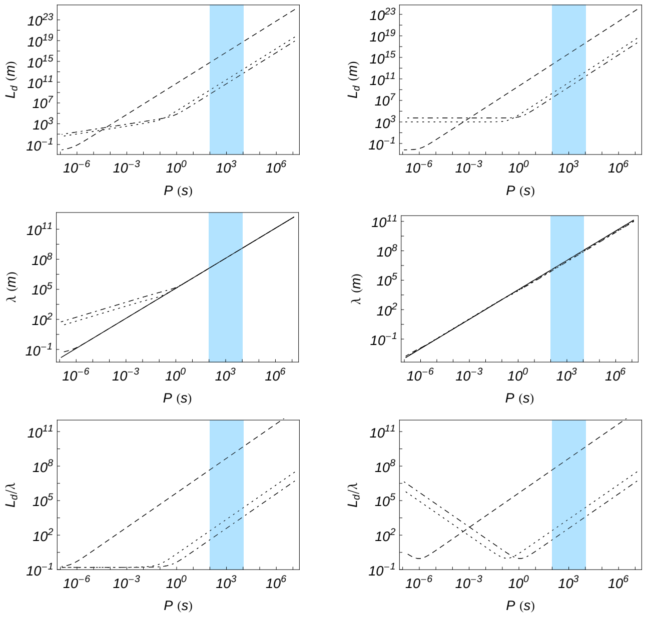

Fig. 2. Damping length, wavelength, and ratio of the damping length to the wavelength versus period for the adiabatic fast (left panels) and slow (right panels) waves in a FIIP (solid), a FIRP (dashed) and a PIP with $\tilde{\mu} = 0.8$ (dotted) and $\tilde{\mu} = 0.95$ (dash-dotted).

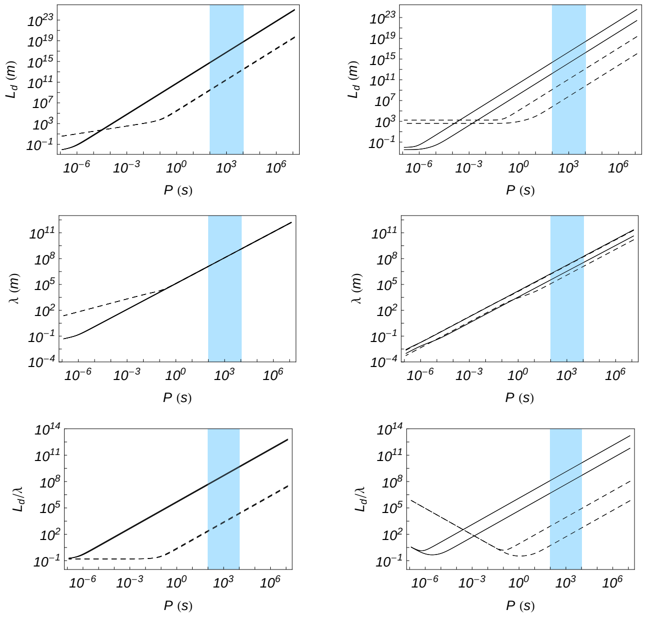

Fig. 3. Damping length, wavelength, and ratio of the damping length to the wavelength versus period for the adiabatic fast (left panels) and slow (right panels) waves in a FIIP (solid) and in a PIP with $\tilde{\mu} = 0.8$ (dashed). The background flow speed is 10 km/s.

$$-4ic_{\mathrm{s}}^2\left[\eta_{\mathrm{C}}\omega - iv_{\mathrm{a}}^2\cos^2\theta - v_{\mathrm{a}}^2\rho_0\Xi(\cos^2\theta - 1)\right]$$

$$C = 2ic_{\mathrm{s}}^2\left[\eta_{\mathrm{C}}\omega - iv_{\mathrm{a}}^2\cos^2\theta - v_{\mathrm{a}}^2\rho_0\Xi(\cos^2\theta - 1)\right]$$

and the wavenumbers are,

$$k_1 = \pm\sqrt{\omega^2 k_{\mathrm{m}}^2} \qquad (39)$$

$$k_2 = \pm\sqrt{\omega^2 k_{\mathrm{n}}^2} \qquad (40)$$

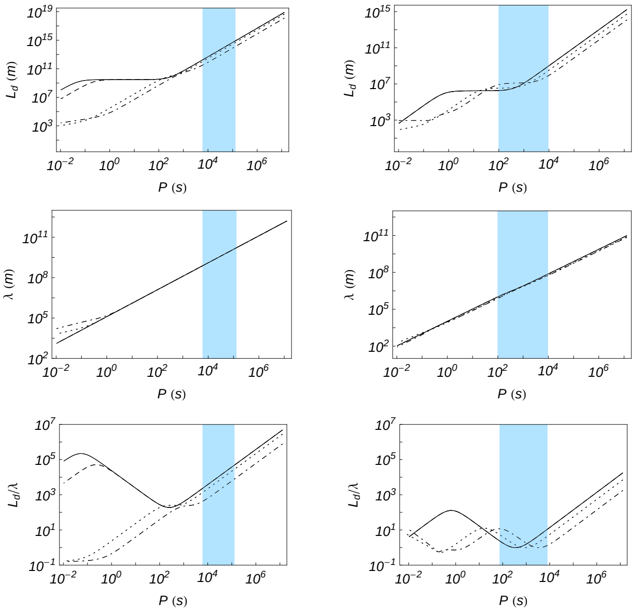

Fig. 4. Damping length, wavelength, and ratio of the damping length to the wavelength versus period for the non-adiabatic fast (left panels), slow (right panels) waves in a FIIP (solid), a FIRP (dashed), and a PIP with $\tilde{\mu} = 0.8$ (dotted) and $\tilde{\mu} = 0.95$ (dash-dotted).

Figure 2 displays the behaviour of damping length, wavelength and the ratio of damping length to wavelength versus period for fast and slow waves in a PIP, respectively. The damping length of both slow and fast waves is severely influenced by ion-neutral collisions showing a strong dependence on the period for periods greater than 1 s while for shorter periods the dependence becomes weaker. This figure also shows that with respect to a FIIP the wavelength of the fast waves is slightly affected by the partial ionisation, deviating from the linear behaviour for periods below 1 s, while the wavelength of slow waves is not affected at all. Within the interval of observed periods in prominence oscillations, when ionisation decreases the ratio between the damping length and the wavelength also decreases for both waves and the spatial damping becomes more efficient. The maximum efficiency of the spatial damping for fast waves is attained for periods below 1 s while for slow waves the maximum of efficiency is attained at a period which depends on the ionisation fraction. The location of this maximum moves towards long periods when the ionisation of the plasma decreases, but when almost neutral plasmas are considered it is still located at a period slightly greater than 1 s, ouside the region of interest. Finally, comparing Figures 1 and 2 it becomes obvious that the behaviour of Alfvén and fast waves is quite similar.

4.2. Adiabatic Magnetoacoustic waves with background flow

Setting $A = H = 0$ in Eq. (20) and substituting in Eq. (19), we obtain the dispersion relation for adiabatic magnetoacoustic waves in a PIP with a background flow, which is

$$(\Omega^2 - k^2 c_{\rm s}^2)(ik^2 \eta_{\rm C} \Omega - \Omega^2) + k^2 v_{\rm a}^2 (\Omega^2 - k_x^2 c_{\rm s}^2) + \\ + ik^2 k_z^2 v_{\rm a}^2 c_{\rm s}^2 \Xi \rho_0 \Omega = 0 \quad (41)$$

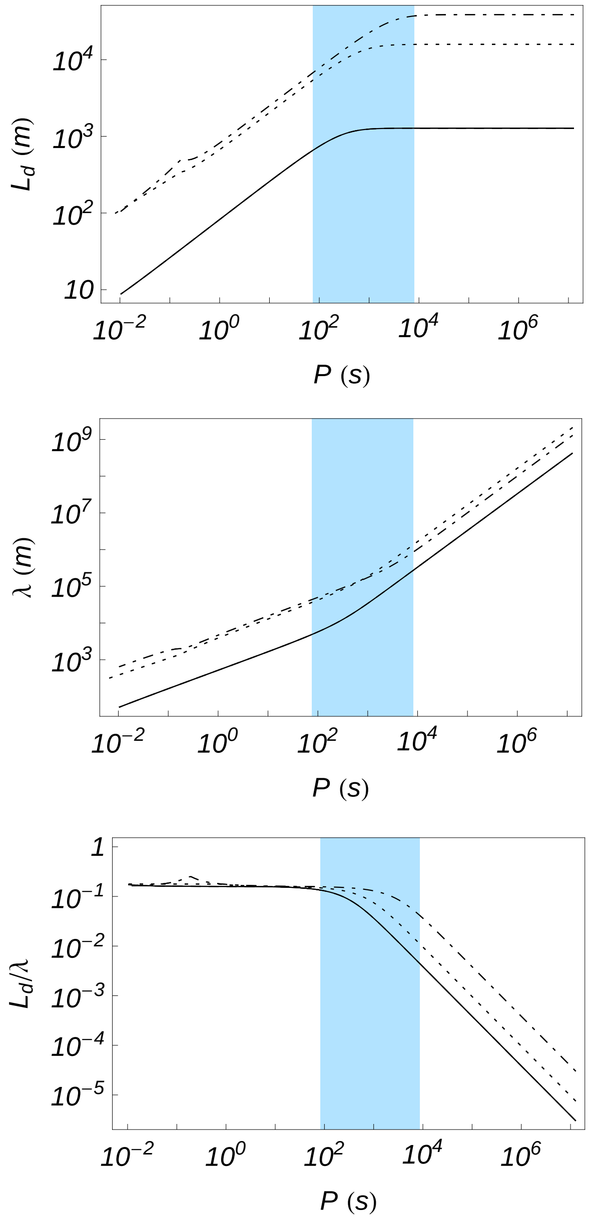

Fig. 5. Damping length, wavelength, and ratio of the damping length to the wavelength versus period for the non-adiabatic thermal wave in a FIIP (solid), a FIRP (dashed), and a PIP with $\tilde{\mu} = 0.8$ (dotted) and $\tilde{\mu} = 0.95$ (dash-dotted).

4.2.1. Fully ionised resistive plasma

Considering FIRP conditions from 2.2, the dispersion relation (41) becomes,

$$(\Omega^2 - k^2 c_\mathrm{s}^2)(ik^2\eta\Omega - \Omega^2) + k^2 v_\mathrm{a}^2(\Omega^2 - k_x^2 c_\mathrm{s}^2) = 0 \tag{42}$$

The dispersion relation is a fifth degree polynomial in the wavenumber k, and for this reason we expect two slow waves and two fast waves which, for the flow speed considered, propagate in opposite directions, plus an additional wave. When only longitudinal propagation is considered, the above dispersion relation becomes,

$$(\Omega^2 - k^2 c_\mathrm{s}^2)\left[k^2(i\eta\Omega + v_\mathrm{a}^2) - \Omega^2\right] = 0 \tag{43}$$

and slow waves are decoupled from fast waves propagating undamped, while fast waves are damped by resistivity. The wavenumbers corresponding to the undamped slow waves are

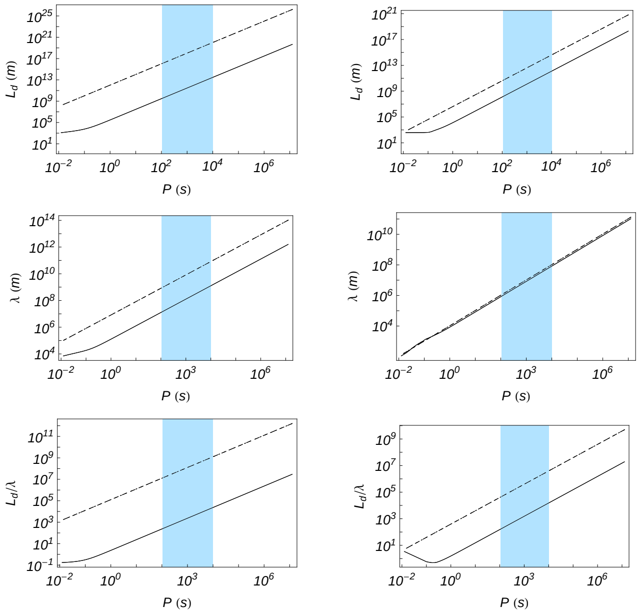

Fig. 6. Damping length, wavelength, and ratio of the damping length to the wavelength versus period for the non-adiabatic fast (left panels), slow (right panels) waves, without radiation, in a FIIP (dashed), a FIRP (dotted) and a PIP with $\tilde{\mu} = 0.8$ (solid).

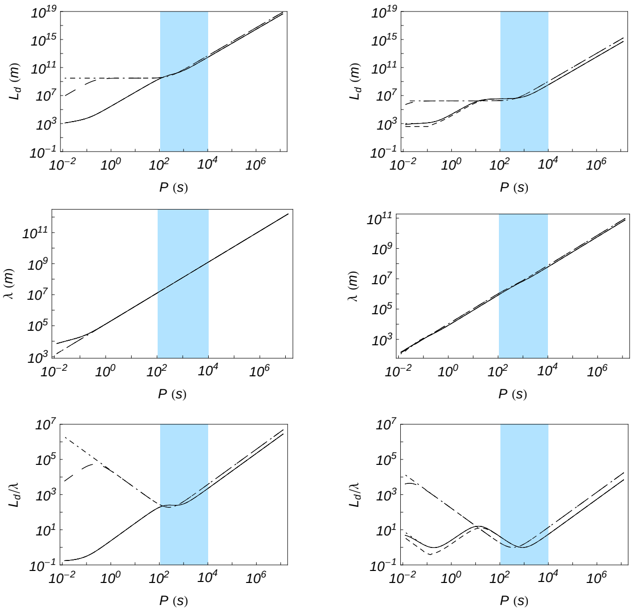

Fig. 7. Damping length, wavelength, and ratio of the damping length to the wavelength versus period for the non-adiabatic fast (left panels), slow (right panels) waves in a PIP ($\tilde{\mu} = 0.8$) without neutrals thermal conduction (solid); without electronic thermal conduction (dashed) and without thermal conduction (dotted); in a FIIP without thermal conduction (dash-dotted), and in a FIRP without thermal conduction (long-dashed).

given by,

$$k = \frac{\omega}{v_0 \pm c_{\rm s}} \tag{44}$$

Concerning the fast waves, now Alfvén waves because of longitudinal propagation, the corresponding dispersion relation, given by the second factor in Eq. (43), is equivalent to Eq. (24) when $\theta = 0$. The solutions to this dispersion relation are given by Eqs. (25)

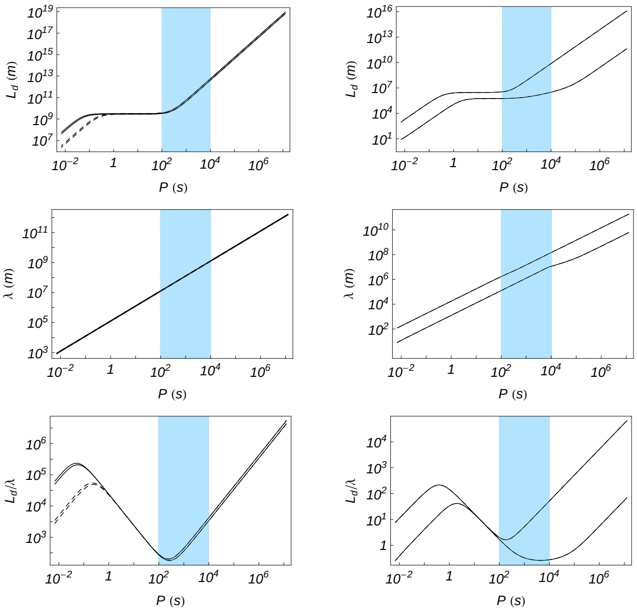

Fig. 8. Damping length, wavelength, and ratio of the damping length to the wavelength versus period for the non-adiabatic fast (left panels), slow (right panels) waves in a FIIP (solid), and in a FIRP (dashed). The flow speed is 10 km/s.

and (28) with $\theta = 0$, and we obtain three Alfvén waves similar to those studied in 3.2. Then, the expected additional wave mentioned above is a fast wave which, for longitudinal propagation and when a background flow is present, becomes the third Alfvén wave already found in 3.2. When oblique propagation is allowed, fast and slow waves become coupled and the dispersion relation (42) is solved numerically. Figure 3 displays the behaviour of the damping length, wavelength and the ratio of the damping length to wavelength versus period for fast and slow waves in a FIRP. Because of the strong difference between Alfvén and flow speeds, in the case of fast waves the unfolding in wavelength and damping length due to the flow is not evident, while for slow waves it is clearly seen. In both cases the behaviour of the wavelength versus period is linear, similar to what happens for a FIIP and the only difference is provided by the unfolding produced by the flow. The damping length also behaves linearly with period and, for slow waves, the unfolding in wavelength and damping length produces two different curves for the ratio $L_{\rm d}/\lambda$. In both curves, the most efficient spatial damping appears for periods far away from those of interest in prominence oscillations. For fast waves, the ratio $L_{\rm d}/\lambda$ behaves linearly with period and its value is very large within the region of periods of interest. The behaviour of the third fast wave is quite different from the other two fast waves and very similar to that of the third Alfvén wave shown in 3.2, being strongly damped within the interval of periods considered.

4.2.2. Partially ionised plasma

Our dispersion relation is given by Eq. (41) which is a fifth degree polynomial in k, and when longitudinal propagation is considered we recover the results of 4.2.1 with slight differences due to the different numerical value of Cowling's resistivity. Such as it is shown in Figure 3, at periods longer than 0.1 s, the damping lengths of both slow and fast waves

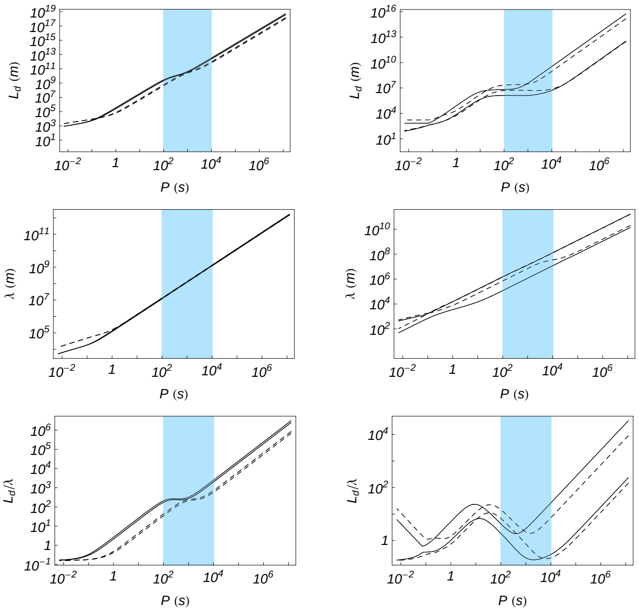

Fig. 9. Damping length, wavelength, and ratio of the damping length to the wavelength versus period for the non-adiabatic fast (left panels), slow (right panels) waves in a PIP with $\tilde{\mu} = 0.8$ (solid) and $\tilde{\mu} = 0.95$ (dashed). The flow speed is 10 km/s.

increase linearly with the period. However, for periods below 0.1 s the damping length slowly decreases in the case of fast waves and becomes constant for slow waves. Furthermore, the wavelength of fast waves for periods below 0.1 s increases with respect to the FIRP case while the wavelengths corresponding to slow waves are only slightly modified. Concerning the ratio of the damping length versus the wavelength, the unfolding in wavelength caused by the flow and the change of the damping length due to the partial ionisation produces that fast waves are much more efficiently attenuated, than in a a FIRP, for any period, but especially at periods below 0.1 s, while for slow waves the peak of maximum efficiency is displaced towards long periods when ionisation decreases, and for almost neutral plasmas would approach the region of periods usually observed in prominence oscillations. Again, the behaviour of the remaining third fast wave is very similar to that found for the third Alfvén wave discussed in 3.2.

In absence of flow the dispersion relation (42) becomes a fourth degree polynomial in k and the third fast wave disappears. Such as it happens for Alfvén waves with a background flow, this third fast wave appears due to the joint action of flow and resistivity, since when a FIIP with a background flow is considered, the dispersion relation also becomes a fourth degree polynomial in k and the third fast wave is absent.

4.3. Non-adiabatic Magnetoacoustic waves in a prominence plasma without background flow

Setting $v_0 = 0$ in expression (5) and substituting in Eq. (19), we obtain the dispersion relation for non-adiabatic magnetoacoustic waves in a PIP without a background flow, which is

$$(\omega^2 - k^2\Lambda^2)(ik^2\eta_{\mathrm{C}}\omega - \omega^2) + k^2 v_{\mathrm{a}}^2(\omega^2 - k_x^2\Lambda^2) + \\ + ik^2 k_z^2 v_{\mathrm{a}}^2 \Lambda^2 \Xi \rho_0 \omega = 0 \qquad (45)$$

4.3.1. Fully ionised resistive plasma

Once imposed the conditions corresponding to a FIRP, the following dispersion relation, a sixth degree polynomial in the wavenumber k, is obtained,

$$(\omega^2 - k^2\Lambda^2)(ik^2\eta\omega - \omega^2) + k^2 v_{\mathrm{a}}^2(\omega^2 - k_x^2\Lambda^2) = 0 \tag{46}$$

which describes coupled fast, slow and thermal waves. When only longitudinal propagation is allowed, the above dispersion relation becomes,

$$(\omega^2 - k^2\Lambda^2)\left[k^2(i\eta\omega + v_{\mathrm{a}}^2) - \omega^2\right] = 0 \tag{47}$$

Then, like in 3.1 we obtain two decoupled Alfvén waves, damped by resistivity, whose dispersion relation is given by,

$$k^2 = \frac{\omega^2}{v_{\mathrm{a}}^2 + i\omega\eta} \tag{48}$$

and another dispersion relation,

$$k^2 = \frac{\omega^2}{\Lambda^2} \tag{49}$$

which is a fourth degree polynomial in k describing coupled propagating thermal and slow waves, only damped by thermal effects. The dispersion relation (46) has been solved numerically and Figures 4 and 5 show the behaviour of the damping length, wavelength and ratio of the damping length to the wavelength versus period for the fast, slow and thermal waves. Starting with Figure 4 we have only considered an interval of periods between 10^{-2} and 10^7 s, since for periods smaller than 10^{-2} s, much shorter than those of interest, the curves become very entangled. In the case of the fast wave, when an FIIP is considered the spatial damping is governed by radiative losses and thermal conduction (Carbonell et al. 2006) in the interval of periods from 10^{-2} to 10^7 s. However, in a FIRP we observe a slight change in the damping length of fast waves around a period of 1 s. This change tells us that the dominance of thermal conduction appears slightly before than in the ideal case. Also, looking to the ratio between the damping length and the wavelength we observe that in this case the efficiency of the damping for fast waves is improved, with respect to a FIIP, for periods below 1 s. For slow waves, no differences appear in the behaviour of FIIP and FIRP. The behaviour of thermal waves (Figure 5) is exactly the same in FIIP and FIRP.

4.3.2. Partially ionised plasma

Now, our dispersion relation is given by Eq. (45) and when only longitudinal propagation is allowed the expression is similar to that of 4.3.1, although the numerical value of the Cowling's resistivity is different and the results for fast waves would be different. When oblique propagation is considered, the dispersion relation (45) has been solved numerically and a strong distortion of the damping length and wavelength curves corresponding to fast waves (Figure 4, left panels) appears. Basically, the changes affect the radiative plateau, between periods 10^3 and 10^{-2} s, and partial ionisation decreases the damping length of fast waves in this region. For slow waves (Figure 4, right panels), a similar behaviour is found in the same regions although the distortion is not so important since a very short radiative plateau, between 10^2 and 10^3 s remains, together with a region, between 1 and 10^2 s, where thermal conduction is dominant. As compared to a FIRP, the ratio L_d/λ for fast waves decreases substantially for periods below 10^3 s, although for the periods of interest in prominences this ratio remains very large. For slow waves, partial ionisation produces that the ratio L_d/λ reaches a maximum of efficiency, ~ 1, for periods similar to those involved in prominence oscillations, and this maximum is displaced towards longer periods when ionisation is decreased. The changes in the wavelengths of slow and fast waves are similar to those shown in the adiabatic case (Sect. 4.1.2). In the case of thermal waves (Figure 5), partial ionisation increases both the damping length and wavelength of these waves, although the behaviour of the ratio L_d/λ is similar to previous cases. Since thermal wave is always strongly damped, which makes its detection very difficult, in the following we will avoid further comments on it.

In order to understand the effects of radiation and thermal conduction by neutrals and electrons, in Figure 6 we represent, for fast and slow waves, the same quantities but with optically thin radiation and heating removed i.e. only thermal conduction is at work, and we can observe that the most efficient damping for both waves occurs for partially ionised plasmas, which suggests that the inclusion of the isotropic thermal conduction due to neutrals plays a very important role for all the periods considered. However, we must take into account that when the ionisation fraction decreases, radiation also decreases and that, because of neutrals, thermal conduction is favoured, what makes difficult to establish meaningful comparisons between plasmas with different degrees of ionisation.

Next, in Figure 7 we plot the behaviour of fast and slow waves, when thermal conduction has been removed i.e. only radiation and heating remain. When thermal conduction by electrons and neutrals is removed, the behaviour of fast waves in a FIIP and in FIRP is similar and, within the interval of periods of interest, the behaviour of the different quantities corresponding to the different types of plasma is the same. However, when periods below 100 s are considered, FIIP and FIRP are strongly affected by the lack of thermal conduction. For slow waves, a similar behaviour appears and the most important conclusion is that when we compare Figures 6 and 7, and within the interval of periods of interest, the presence of a very efficient damping is due to optically thin radiation.

On the other hand, when non-adiabatic magnetoacoustic waves are considered, the importance of radiation and thermal conduction can be also quantified in terms of two dimensionless parameters (De Moortel and Hood 2004), namely, the thermal ratio, which modified for the case of partial ionisation becomes,

$$d = \frac{(\gamma-1)(\kappa_{\mathrm{e}\parallel}+\kappa_\mathrm{n})T_0\rho_0}{\gamma^2 p_0^2 \tau_\mathrm{s}} = \frac{1}{\gamma}\frac{\tau_\mathrm{s}}{\tau_\mathrm{cond}}, \tag{50}$$

which is $1/\gamma$ times the ratio of the sound travel time ($\tau_\mathrm{s} = l/c_\mathrm{s}$) to the thermal conduction timescale ($\tau_\mathrm{cond} = l^2 p_0 / \left[(\gamma-1)(\kappa_{\mathrm{e}\parallel}+\kappa_\mathrm{n})T_0\right]$), and the radiation ratio,

$$r = \frac{(\gamma-1)\tau_\mathrm{s}\xi_i\rho_0^2\chi^* T_0^\alpha}{\gamma p_0} = \frac{\tau_\mathrm{s}}{\tau_\mathrm{r}}, \tag{51}$$

which is the ratio of the sound travel time to the radiation timescale ($\tau_{\rm r} = \gamma p_0 / \left[(\gamma-1)\xi_i \rho_0^2 \chi^* T_0^\alpha\right]$). From the equilibrium parameters, we can compute the value of l at which the condition $d = r$ is satisfied,

$$l = \sqrt{\frac{\kappa_{\rm e\parallel} + \kappa_{\rm n}}{\xi_i \rho_0^2 \chi^* T_0^{\alpha-1}}} \tag{52}$$

where $\kappa_{e\parallel}$ and κ_n are the thermal conduction coefficients corresponding to anisotropic electronic and isotropic, by neutrals, thermal conduction, respectively. Then, when the spatial length of the perturbation, the wavelength, is of the order of l or smaller, thermal conduction becomes dominant. For the slow wave, Figure 4 (Right panels) shows that the transition from a regime dominated by radiation to another dominated by conduction can be clearly seen in the plot of the damping length versus period. For a FIIP, this transition occurs at a period of 1 s while for a PIP, with $\tilde{\mu} = 0.8$, occurs at a period between 10 and 100 s, and with $\tilde{\mu} = 0.95$, occurs at a period close to 100 s. Using the values assumed for prominence parameters, for FIIP we obtain $l \approx 4700$ m; for a PIP ($\tilde{\mu} = 0.8$), $l \approx 40000$ m; and for a PIP ($\tilde{\mu} = 0.95$), $l \approx 100000$ m. Then, setting these periods in the plot of the wavelength versus period in Figure 4 (Right panels), we can check that the numerical value of the wavelength is almost coincident with the above analytical determinations for l. The reason for this increase in the numerical value of l is that for a PIP thermal conduction is enhanced due to neutrals contribution, increasing when the ionisation fraction decreases, while the denominator of l decreases when the ionisation fraction decreases. Summarizing, when ionisation decreases the period at which the dominant damping mechanism changes from radiation to thermal conduction increases and, consequently, the wavelength also increases.

4.4. *Non-adiabatic Magnetoacoustic waves in a prominence plasma with background flow*

4.4.1. Fully ionised ideal plasma

Setting in Eq. (19) conditions corresponding to FIIP, we obtain,

$$(\Omega^2 - k^2\Lambda^2)(-\Omega^2) + k^2 v_{\rm a}^2(\Omega^2 - k_x^2\Lambda^2) = 0 \tag{53}$$

which is a sixth degree polynomial in the wavenumber k. When only longitudinal propagation is allowed, we obtain two undamped Alfvén waves given by,

$$k^2 = \frac{\Omega^2}{v_{\rm a}^2} \tag{54}$$

whose solutions for the wavenumbers are

$$k = \frac{\omega}{v_0 \pm v_{\rm a}} \tag{55}$$

as in Carbonell et al. (2009), while the dispersion relation,

$$\Omega^2 = k^2\Lambda^2 \tag{56}$$

describes coupled slow and thermal waves modified by the flow and damped by thermal effects. In the case of oblique propagation, dispersion relation (53) has been solved numerically and the behaviour of fast and slow waves is shown in Figure 8. When a flow is present the unfolding of wavelengths and damping lengths appears. Since the considered flow speed is much smaller than Alfvén speed, the separation of the curves corresponding to the fast wave is very small while, since flow speed and sound speed are comparable, the curves corresponding to slow waves substantially separate. This effect strongly affects the behaviour of the damping length versus wavelength for slow waves, since one of them has a very efficient spatial damping for periods observed in prominence oscillations. In the case considered in this section, the damping of fast and slow waves is strictly due to thermal effects.

4.4.2. Fully ionised resistive plasma

In this case, considering FIRP conditions, the dispersion relation becomes

$$(\Omega^2 - k^2\Lambda^2)(ik^2\eta\Omega - \Omega^2) + k^2 v_{\mathrm{a}}^2(\Omega^2 - k_x^2\Lambda^2) = 0 \tag{57}$$

which is a seventh degree polynomial in the wavenumber k. Considering only longitudinal propagation, we find, again, coupled slow and thermal waves modified by the flow and damped by thermal effects, and three Alfvén waves given by the dispersion relation (24), with $\theta = 0$, and its solutions. Therefore, when we solve dispersion relation (57), we expect three fast, two slow and two thermal propagating waves. In Figure 8 fast and slow waves have been plotted and compared with the previous case. Such as it is shown, for fast and slow waves no important differences in the behaviour with respect to the ideal case are seen. Thermal waves, as well as the third fast wave, are strongly damped after a very short distance.

4.4.3. Partially ionised plasma

Now, the dispersion relation is given by Eq. (19) and Figure 9 displays the behaviour of the damping length, wavelength and ratio of damping length versus wavelength for fast and slow waves. The most interesting results are those related with the ratio L_{d}/λ. For fast waves, this ratio decreases with the period becoming small for periods below 10^{-2} s while for one of the slow waves, the ratio becomes very small for periods typically observed in prominence oscillations. When ionisation is decreased, slight changes of the above described behaviour occur, the most important being the displacement towards longer periods of the peak of most efficient damping corresponding to slow waves. Such as it has been pointed out before, the presence of a third fast wave is, again, due to the joint action of flow and resistivity. In absence of flow or resistivity, the dispersion relation would become a sixth order polynomial in the wavenumber and this wave would be absent.

5. Conclusions

Quiescent solar prominences and filaments are partially ionised plasmas and some of their typical features are the presence of material flows and oscillations. While the time damping of these oscillations has been thoroughly studied, their spatial damping demands an in-depth study. Interpreting the observed oscillations in terms of MHD waves, we have analysed the spatial damping of Alfvén and non-adiabatic magnetoacoustic waves in a flowing partially ionised prominence plasma. Several different cases, with dispersion relations of increasing complexity, have been considered, and the conclusions derived from our study are summarised in the following.

As it is well known, Alfvén waves are difficult to damp since non-adiabatic effects do not affect them, however, when Alfvén waves in a partially ionised plasma are considered, they can be spatially damped and analytical expressions describing their spatial damping can be obtained. When the ionisation decreases, the damping length of these waves also decreases and the efficiency of their spatial damping in the range of periods of interest is improved, although the most efficient damping is attained for periods below 1 s. A new feature is that when a flow is present a new third Alfvén wave, strongly attenuated, appears. The presence of this wave depends on the joint action of flow and resistivities, since in absence of flow, or for a FIIP, the dispersion relation becomes quadratic giving place to the two well-known Alfvén waves. Furthermore, this third wave could only be detected by an observer not moving with the flow.

When adiabatic magnetoacoustic waves are considered and the effect of partial ionisation is taken into account, some new features appear. When a FIRP is considered and only longitudinal propagation is allowed, slow waves are decoupled from fast waves, propagating undamped while fast waves propagate with a modified Alfvén speed and are damped by resistivity. When a PIP plasma is studied and only longitudinal propagation is allowed, the same happens but now the numerical value of Cowling's resistivity is greater than before enhancing the damping. Then, the behaviour of slow waves is only influenced by partial ionisation when oblique propagation is allowed. Furthermore, when a PIP is considered the behaviour of fast waves is very similar to that of Alfvén waves and the damping becomes very efficient for periods below 1 s, while for slow waves the peak denoting the most efficient damping moves towards higher periods when the plasma ionisation decreases. When in the adiabatic case a flow is considered, the main difference is the unfolding of the damping length, wavelength and damping length to wavelength curves, and the apparition of a third fast wave, strongly damped, due to the join presence of flow and resistivities.

Considering now non-adiabatic magnetoacoustic waves, when partial ionisation is present the behaviour of fast, slow and thermal waves is strongly modified. Comparing with non-adiabatic fast waves in a FIIP, which are damped by electronic thermal conduction and radiation, the damping length of a fast wave in a PIP is strongly diminished by neutrals thermal conduction for periods between 0.01 and 100 s, and, at the same time, the radiative plateau present in FIIP and FIRP disappears. The behaviour of slow waves is not so strongly modified as for fast waves, although thermal conduction by neutrals also diminishes the damping length for periods below 10 s, and a short radiative plateau still remains for periods between 10 and 1000 s. Finally, thermal waves are only slightly modified although the effect of partial ionisation is to increase the damping length of these waves, just the opposite to what happens with the other waves. Next, when a background flow is included, a new third fast wave appears which, again, is due to the joint action of flow and resistivities. As we already know, wavelengths and damping lengths are modified by the flow, and since for slow waves sound speed and observed flow speeds are comparable this means that the change in wavelength and damping length are important leading to an improvement in the efficiency of the damping. Also, the maximum of efficiency is displaced towards long periods when the ionisation decreases, and for ionisation fractions from 0.8 to 0.95 it is clearly located within the range of periods typically observed in prominence oscillations with a value of $L_{\rm d}/\lambda$ smaller than 1. This means that for a typical period of 10^3 s, the damping length would be between 10^2 and 10^3 km, the wavelength around 10^3 km and, as a consequence, in a distance smaller than a wavelength the slow wave would be strongly attenuated. On the other hand, during our calculations we have found that the different heating mechanisms usually considered (Carbonell et al. 2004) do not affect the results.

In conclusion, the joint effect of non-adiabaticity, flows and partial ionisation allows slow waves to damp in an efficient way within the interval of periods typically observed in prominences. Thermal waves are attenuated very efficiently within the interval of interest but, probably, their observational detection is very difficult, and fast waves are very unefficiently atenuated within the considered interval. Furthermore, since Alfvén and fast waves display a similar behaviour, the observational discrimination between them should be based on the detection of their associated perturbations. It is also important to remark that the new fast and Alfvén waves are only detectable in a reference system external to the flow, however, its short damping length should make its detection very difficult. Such as we have seen, even in the most simple case of an unbounded medium threaded by a uniform magnetic field, the inclusion of non-adiabatic effects, partial ionisation and flows complicates the study of the spatial damping of prominence oscillations because of the apparition of new waves and the difficulty to discriminate between the different effects. This also points out that from observations, and due to the entanglement of the different effects, it is extremely difficult to properly interpret the observed oscillations in terms of MHD waves.

The present study represents a first step in the investigation of the behaviour of the spatial damping of MHD waves in partially ionised prominence plasmas. Forthcoming studies must focus in investigating the behaviour of this type of damping in fine structures, threads, which we think are the basic constituents of quiescent prominences.

Acknowledgements

The authors acknowledge the financial support provided by MICINN and FEDER funds under grant AYA2006-07637. P. Forteza acknowledges a FPU fellowship from MECyT. Also, the Conselleria d'Economia, Hisenda i Innovació of the Government of the Balearic Islands is gratefully acknowledged for the funding provided under grant PCTIB2005GC3-03.

References

Arregui, A., Terradas, J., Oliver, R., & Ballester, J. L. 2008, ApJ, 682, L141

Banerjee, D., Erdélyi, R., Oliver, R., & O'Shea, E. 2007, Sol. Phys., 246, 3

Berger, T. E., Shine, R. A., Slater, G. L.,Tarbell, T. D., Title, A. M. Okamoto, T. J.; Ichimoto, K., Katsukawa, Y., Suematsu, Y., Tsuneta, S., Lites, B., Shimizu, T. 2008, ApJ, 676, L89

Braginskii, S. I. 1965, Rev. Plasma Phys., 1, 205

Carbonell, M., Oliver, R., & Ballester, J. L. 2004, A&A, 415, 739

Carbonell, M., Terradas, J., Oliver, R., & Ballester, J. L. 2006, A&A, 460, 573

Carbonell, M., Oliver, R., & Ballester, J. L. 2009, New A,14, 277

De Moortel, I., Hood, A. W., Ireland, J., & Walsh, R. W. 2002, Sol. Phys., 209, 89

De Moortel, I. & Hood, A. W. 2003, A&A, 408, 755

De Moortel, I. & Hood, A. W. 2004, A&A, 415, 705

De Pontieu, B., Martens, P. C. H., & Hudson, H. S. 2001, ApJ, 558, 859

Forteza, P., Oliver, R., Ballester, J. L., & Khodachenko, M. L. 2007, A&A, 461, 731

Forteza, P., Oliver, R., & Ballester, J. L. 2008, A&A, 492, 223

Gilbert, H. R., Hansteen, V. H., & Holzer, T. E. 2002, A&A, 577, 464

Gilbert, H., Kilper, G., & Alexander, D. 2007, ApJ, 671, 978

Goedbloed, H. & Poedts, S. 2004, Principles of Magnetohydrodynamics. Cambridge University Press

Kulsrud, R., & Pearce, W. P. 1969, ApJ, 156, 445

Khodachenko, M. L., Arber, T. D., Rucker, H. O., & Hanslmeier, A. 2004, A&A, 422, 1073

Labrosse, N., Heinzel, P., Vial, J. V., Kucera, T., Parenti, S., Gunár, S., Schmieder, B. & Kilper, G. 2009, Space Sci. Rev., (submitted)

Leake, J. E., Arber, T. D., & Khodachenko, M. L. 2005, A&A, 442, 1091

Lin, Y., Engvold, O., & Wiik, J. E. 2003, Sol. Phys., 216, 109

Lin, Y., Engvold, O., Rouppe van der Voort, L. H. M., & van Noort, M. 2007, Sol. Phys., 246, 65

Mackay, D., Karpen, J., Ballester, J. L., Schmieder, B., & Aulanier, G. 2009, Space Sci. Rev.(submitted)

Mercier, C. & Heyvaerts, J. 1977, A&A, 61, 685

Okamoto, T. J, et al. 2007, Science, 318, 1557

Oliver, R. 2009, Space Sci. Rev.(In press)

Oliver, R. & Ballester, J. L. 2002, Sol. Phys., 206, 45

Patsourakos, S, & Vial, J.-C. 2002, Sol. Phys., 208, 253

Singh, K. A. P. 2006, JApA, 27, 321

Singh, K. A. P., Dwivedi, B. N., Hasan, S. S. 2007, A&A, 473, 931

Singh, K. A. P., Krishan, V. 2009, New A, in press

Soler, R., Oliver, R., & Ballester, J. L. 2008, ApJ, 684, 725

Soler, R., Oliver, R., & Ballester, J. L. 2009a, ApJ, 693, 1601

Soler, R., Oliver, R., & Ballester, J. L. 2009b, ApJ, 695, L166

Soler, R., Oliver, R., & Ballester, J. L. 2009c, ApJ, 699, 1553

Soler, R., Oliver, R., & Ballester, J. L. 2009d, In preparation

Tanenbaum, B. S. 1961, Phys. Fluids, 4, 1262

Tanenbaum, B. S., & Mintzer, D. 1962, Phys. Fluids, 5, 1226

Terradas, J., Molowny-Horas, R., Wiehr, E., et al. 2002, A&A, 393, 637

Terradas, J., Carbonell, M., Oliver, R., & Ballester, J. L. 2005, A&A, 434, 741

Watanabe, T. 1961a, Can. J. Phys., 39, 1044

Watanabe, T. 1961b, Can. J. Phys., 39, 1197

Watts, C., & Hanna, J. 2004, Phys. Plasmas, 11, 1358

Woods, L. C. 1962, J. Fluid Mechanics, 13, 570

Zirker, J. B., Engvold, O., & Martin, S. F. 1998, Nature, 434, 741